Post-print version of the following article published in the Journal of Cell Science

DAZL and CPEB1 regulate mRNA translation synergistically during oocyte maturation

Joao P Sousa Martins [1], Xueqing Liu [1], Ashwini Oke [2], Ripla Arora [1], Federica Franciosi [3], Stephan Viville [4], Diana J Laird [1], Jennifer C Fung [2], Marco Conti [5]

Affiliations

[1] Center for Reproductive Sciences, University of California, San Francisco, CA 94143, USA Eli and Edythe Broad Center of Regeneration Medicine and Stem Cell Research, University of California, San Francisco, CA 94143, USA Department of Obstetrics and Gynecology and Reproductive Sciences, University of California, San Francisco, CA 94143, USA.
[2] Center for Reproductive Sciences, University of California, San Francisco, CA 94143, USA Department of Obstetrics and Gynecology and Reproductive Sciences, University of California, San Francisco, CA 94143, USA Department of Biochemistry and Biophysics, University of California, San Francisco, CA 94143, USA.
[3] Center for Reproductive Sciences, University of California, San Francisco, CA 94143, USA Eli and Edythe Broad Center of Regeneration Medicine and Stem Cell Research, University of California, San Francisco, CA 94143, USA Department of Obstetrics and Gynecology and Reproductive Sciences, University of California, San Francisco, CA 94143, USA Reproductive and Developmental Biology Laboratory, Department of Health, Animal Science and Food Safety, Università degli Studi di Milano, 20133, Milano, Italy.
[4] Institut de Génétique et Biologie Moléculaire et Cellulaire (IGBMC), Institut National de Santé et de Recherche Médicale INSERM U964, Centre National de Recherche Scientifique CNRS UMR 1704, Université de Strasbourg, Illkirch 67404, France Centre Hospitalier Universitaire, Strasbourg F-67000, France.
[5] Center for Reproductive Sciences, University of California, San Francisco, CA 94143, USA Eli and Edythe Broad Center of Regeneration Medicine and Stem Cell Research, University of California, San Francisco, CA 94143, USA Department of Obstetrics and Gynecology and Reproductive Sciences, University of California, San Francisco, CA 94143, USA contim@obgyn.ucsf.edu.

Journal of Cell Science 15;129(6):1271-82. doi: 10.1242/jcs.179218.
Submitted: August 17, 2015 Accepted: January 27, 2016 Published: March 15, 2016

ABSTRACT
Meiotic progression requires exquisitely coordinated translation of maternal messenger (m)RNA that has accumulated during oocyte growth. A major regulator of this program is the cytoplasmic polyadenylation element binding protein 1 (CPEB1). However, the temporal pattern of translation at different meiotic stages indicates the function of additional RNA binding proteins (RBPs). Here, we report that deleted in azoospermia-like (DAZL) cooperates with CPEB1

to regulate maternal mRNA translation. Using a strategy that monitors ribosome loading onto endogenous mRNAs and a prototypic translation target, we show that ribosome loading is induced in a DAZL- and CPEB1-dependent manner, as the oocyte reenters meiosis. Depletion of the two RBPs from oocytes and mutagenesis of the 3′ untranslated regions (UTRs) demonstrate that both RBPs interact with the Tex19.1 3′ UTR and cooperate in translation activation of this mRNA. We observed a synergism between DAZL and cytoplasmic polyadenylation elements (CPEs) in the translation pattern of maternal mRNAs when using a genome-wide analysis. Mechanistically, the number of DAZL proteins loaded onto the mRNA and the characteristics of the CPE might define the degree of cooperation between the two RBPs in activating translation and meiotic progression.

KEY WORDS: Oocyte maturation, RBPs, Translation control, DAZL, CPEB

INTRODUCTION

During oocyte growth, when the oocyte arrests in prophase of meiosis I (prophase I), it is highly active transcriptionally, accumulating large amounts of mRNA that are later required for the oocyte-to-zygote transition. A large proportion of transcripts – an estimated 30% in mouse and human – are stored in repressing complexes (Pique et al., 2008; Gosden and Lee, 2010), and are used later during oocyte maturation and early embryo development when transcription is silent. Indeed, transcripts coding for crucial meiotic and cell cycle regulators, including the components of the maturation-promoting factor (MPF), accumulate during oocyte growth but are only translated during oocyte maturation (McGrew and Richter, 1990; Sheets et al., 1994). Consequently, meiotic resumption and progression to the metaphase stage of meiosis II (MII), pronucleus formation, syngamy and the first stages of embryo cleavage are almost completely dependent upon translation control of maternal messages synthesized during oocyte growth. Maternal mRNAs that have accumulated during oocyte growth are remarkably stable, with an estimated half life of 8–12 days (Brower et al., 1981; Clarke, 2012), but upon the first embryo division, over 90% of these mRNAs are degraded (Hamatani et al., 2004).

Two pivotal regulatory structures of eukaryotic translation are located at opposite ends of the mRNA – the 7-methylguanylate (m7G) cap at the 5′ end and the poly(A) tail at the 3′ end. Regulatory elements within the mRNA use these two structures to repress and activate translation in a concerted manner throughout oocyte maturation. One central mechanism for regulating maternal mRNAs relies on the dynamic modulation of the poly(A) tail, which is located at the 3′ end of the mRNA, where polyadenylation of silent messages is associated with activation of translation (Radford et al., 2008; Brook et al., 2009). The cytoplasmic polyadenylation element (CPE) is a consensus U-rich sequence [UUUUA(A)U] located within the 3′ UTR of mRNAs. CPEs complex with CPE-binding proteins (CPEBs) and, through recruitment of different protein partners, promote translation repression or activation. In dormant transcripts, CPEB represses translation by preventing the assembly of the cap complex and by recruiting proteins that either compete for cap binding with eukaryotic initiation

factor 4E (eIF4E) or that compete with eIF4G for an interaction with eIF4E (e.g. Maskin, 4EBP and CUP). Additionally, in immature frog oocytes, CPEB recruits the poly(A) ribonuclease (PARN) and the germline development factor 2 (GLD2) simultaneously, in order to maintain a short poly(A) tail (Cao and Richter, 2002; Kim and Richter, 2006; Fernandez-Miranda and Mendez, 2012). Upon reentry into meiosis, phosphorylation of CPEB releases PARN, resulting in an increase in poly(A) size that is mediated by GLD2 and concomitant translation of previously dormant messages (Kim and Richter, 2006, 2007). A combinatorial code that determines the extent and timing of translation based on the positions of CPEs and Pumilio-binding elements in respect to the polyadenylation signal on cyclin mRNAs (Cyclin-B1–Cyclin-B5; Cyclin B1 is encoded by CcnB1) has furthered understanding in the activation of translation during MI (Pique et al., 2008).

Recently, a genome-wide analysis of transcripts that are regulated during mouse oocyte maturation identified the RNA-binding protein (RBP) deleted in azoospermia-like (DAZL) as a regulator of translation (Chen et al., 2011). DAZL is fundamental for gametogenesis both in males and females because loss-of-function results in complete abrogation of gametes in both sexes (Ruggiu et al., 1997; Saunders et al., 2003). This RBP regulates translation by binding to a U-rich region within the 3′ untranslated region (UTR) of specific transcripts and promotes translation activation by providing a scaffold for the canonical translation regulator PABP independently of the poly(A) tail (Collier et al., 2005; Jenkins et al., 2011). In mammals, in vivo targets of this protein have been identified both in males and females (Reynolds et al., 2005, 2007; Chen et al., 2011). A positive regulatory loop, where CPEB1 promotes the translation of DAZL, which in turn activates its own translation, has been described in mouse (Chen et al., 2011) and in zebrafish (Takeda et al., 2009).

Work in Xenopus has provided important clues on the mechanisms that are employed to regulate translation and concomitant oocyte maturation, but little is known about these processes in mammals. Previous strategies to study translation in mammalian meiosis have been hindered by the limited amounts of material available; therefore, meiotic stage specific characterization of translational dynamics in the maturing oocyte has not been reported. Using a mouse line expressing an epitope-tagged ribosomal protein (RiboTag), which is activated by the tissue-specific cre recombinase, we recovered transcripts that are associated with ribosomes by using immunoprecipitation. This provides a powerful tool to develop temporally specific profiles of rapid cell-stage transitions (Sanz et al., 2009, 2013). Through the use of RiboTag RNA immunoprecipitation (RIP), together with mutagenesis and bioinformatics analysis, we discovered a close synergy between the two RBPs CPEB1 and DAZL in their function as translation regulators of transcripts during mammalian oocyte maturation. Using a candidate approach, we show that both proteins are required for translation and oocyte meiotic progression.

RESULTS

Ribosome RIP as a strategy to monitor ribosome loading onto maternal mRNAs and translation in the oocyte

A genome-wide analysis of actively translating mRNA during mammalian oocyte maturation provided a first insight into the mechanisms controlling specific translation from transition from prophase I to MI and MII (Chen et al., 2011). However, the large number of oocytes needed for polysome fractionation on a sucrose density gradient limits the temporal resolution of measurements. To circumvent this obstacle, we devised a new strategy to monitor ribosome loading onto oocyte maternal transcripts. We used a mouse model carrying a cre-recombinase-activated hemagglutinin (HA)-labeled ribosomal protein L22 (Rpl22HA; RiboTag) (Sanz et al., 2009, 2013). We surmised that RIP of ribosomes followed by detection of associated mRNA by using quantitative (q)PCR would more efficiently detect ribosome loading onto mRNAs than the use of polysome fractionation. To express RiboTag in oocytes, the Rpl22HA transgenic mice were mated with mice expressing a cre-recombinase under the control of the zona pellucida 3 (Zp3-cre) promoter, which is exclusively expressed in the growing oocyte before the completion of the first meiotic division (de Vries et al., 2000). The selective expression of the tagged ribosomal subunit in the oocyte was confirmed with immunocytochemistry analysis (Fig. 1A,B) and by western blotting (Fig. S1A). HA-tagged ribosomes were expressed throughout the primordial-to-primary follicle transition and persisted throughout oocyte growth (Fig. S1B).

Using the polysome array strategy, we have previously defined three classes of maternal mRNA in the maturing oocyte: class I, representing transcripts constitutively associated with the polysomes; class II, which includes transcripts that dissociate from the polysomes during oocyte maturation; and class III, including transcripts that progressively associate with polysomes as maturation proceeds (Chen et al., 2011). We tested whether representative members of each class [Gdf9=Class I, Paip2=Class II and Tex19.1=Class III (Chen et al., 2011)] behave in similar ways in the RiboTag RIP. As shown in Fig. 1C,D, comparable patterns of RNA–ribosome interaction were observed with polysome arrays and RiboTag RIP. Importantly, RiboTag RIP reduced the material needed by one order of magnitude, from 500–1000 oocytes required for separation on a sucrose gradient to 50–100 for analysis using RiboTag RIP.

Specific maternal mRNAs are differentially translated in a temporal fashion during Xenopus oocyte maturation, and these temporal patterns are crucial for progression through meiosis (Pique et al., 2008). However, little information is available on temporally distinct patterns of translation for the mouse. Given the sensitivity of RiboTag RIP, we used this strategy to determine whether high-resolution time courses of ribosome loading onto mRNA could be generated in mouse oocytes. Oocytes from Zp3-RiboTag mice were matured in vitro, collected throughout meiotic progression and used for RiboTag RIP followed by qPCR. In agreement with previously obtained polysome array data (Chen et al., 2011), we found a constitutive ribosome association with the mRNA coding for Dppa3 throughout oocyte maturation (Fig. S1C), a maternal factor essential in the zygote (Fig. 1E). Conversely, after 2 h of maturation, the mRNA coding for Tex19.1, a suppressor of transposon activation (Ollinger et al., 2008; Reichmann et al., 2013; Tarabay et al., 2013), became progressively associated with ribosomes up to the MII stage (Fig. 1E). This progressive ribosome loading

occurred in the absence of significant changes in the total Tex19.1 levels in the oocyte (Fig. 1E).

To determine whether the ribosome loading onto Tex19.1 reflects an increase in translation, we injected oocytes with a reporter construct containing the 3′ UTR of Tex19.1 fused to the Renilla luciferase open reading frame (ORF) (Fig. S2A). By measuring luciferase accumulation throughout maturation, we observed that the accumulation of the reporter (Fig. 1F) closely followed the ribosome loading onto the endogenous mRNA (Fig. 1E). More importantly, a tenfold increase in TEX19.1 endogenous protein accumulation was detected during maturation by western blotting oocyte extracts (Fig. 1F, inset). These findings are consistent with the prediction that ribosome loading promotes Tex19.1 translation and confirm that ribosome association can be used as a proxy for translation of endogenous mRNAs. Luciferase activity and ribosome loading did not increase significantly when oocytes were maintained at the germinal vesicle stage (Fig. S2C), indicating that translation of the Tex19.1 mRNA is cell cycle dependent.

These initial experiments establish RiboTag RIP as a powerful tool for the detailed analysis of the mechanisms underlying translational regulation during meiotic progression in mammalian oocytes.

RBPs control ribosome loading and translation of Tex19.1

Computational analysis of the 3′ UTR of Tex19.1 identified two potential classes of translational control elements – a non-consensus CPE (UUUUACU), which is present 51 nucleotides upstream of the polyadenylation hexanucleotide (AAUAAA), and three putative DAZL-binding sites (consensus UU[G/C]UU Fig. S2A and D). [It must be noted that the first DAZL putative binding site can actually be subdivided into two overlapping binding consensus sequences, as we have previously reported (Chen et al., 2011). Here, these two overlapping sites have been treated as a single site (Fig. S2A,D).] To determine whether CPEB1 and DAZL are required for the translation of Tex19.1 as well as oocyte maturation, we employed morpholino oligonucleotide (MO) knockdown. Injection of a morpholino against Dazl (DAZL-MO) was performed in DAZL heterozygous (DAZL+/−) oocytes in order to maximize protein depletion. Western blot analysis (Fig. S3A,D) revealed that MO injection caused a 50 and 90% decrease in the endogenous CPEB1 and DAZL protein levels, respectively. The knockdown of CPEB1 was associated with a reduction in the number of oocytes that reached MII after 17 h of in vitro maturation, whereas depletion in DAZL resulted in an almost complete block of progression into MII (Fig. S3B,E). We then used the RiboTag RIP protocol to evaluate the consequence of depleting these RBPs on ribosome loading onto the endogenous mRNAs. We observed a significant decrease in ribosome recruitment to the Tex19.1 and Ccnb1 mRNAs after injection of the morpholino targeting CPEB1 (CPEB1-MO) (Fig. 2A). CcnB1 is a canonical CPEB1 target (Sheets et al., 1994; Pique et al., 2008); conversely, knockdown of CPEB1 had no effect on Rpl19 loading (Fig. 2A). A DAZL concentration-dependent decrease in ribosome loading onto Tex19.1 mRNA was proportional to the depletion of DAZL (Fig. 2B). We observed no effect of the

DAZL knockdown on CcnB1 or Rpl19 (Fig. 2B). These data show that disruption of ribosome loading onto mRNA is RBP-specific because CcnB1 is only affected by knockdown of CPEB1, whereas Tex19.1 requires both RBPs for ribosome recruitment. Depletion of either RBP had no effect on total transcript levels, ruling out a possible destabilizing effect (Fig. S3C,F).

Upon injection of the *Tex19.1* reporter into control and RBP-depleted oocytes, luciferase accumulation decreased in parallel to the decrease in ribosome loading onto the endogenous mRNA (Fig. 3A,B). However, although an increase in reporter translation rate clearly continued to be present at 4–6 h in CPEB1-depleted oocytes, the reporter accumulation after DAZL depletion was monotonic (single translation rate) (Fig. 3B; Fig. S4). An assessment of translation beyond 8 h would not be informative because oocytes depleted of these proteins failed to reach the MII stage (Fig. S3B,E). We also noted a small but significant increase in reporter accumulation when either CPEB1 or DAZL were depleted from the germinal vesicle oocytes (Fig. 3C,D). This finding suggests that these two RBPs could also contribute to the repression of *Tex19.1* translation in quiescent germinal vesicle oocytes.

CPEB1 regulates Tex19.1 translation through a non-consensus CPE

Cytoplasmic polyadenylation is key to translation during gametogenesis (Hake and Richter, 1994), and CPEs are associated with regulation of the poly(A) tail. A similar element is present in the 3′ UTR of Tex19.1 (Fig. S2A and D), suggesting polyadenylation as a regulatory mechanism for the translation of this mRNA. Of note, the results from the polysome recruitment and the luciferase reporter suggest that if polyadenylation regulates translation of Tex19.1, this should occur after the germinal vesicle stage but before the MI stage. Indeed, analysis of the endogenous Tex19.1 mRNA with a poly(A) tail (PAT) assay revealed elongation during the first meiotic division (Fig. 4). We detected an increase in polyadenylation from, on average, 150 to 200 adenosine residues, indicating a direct role for CPEB1 in the translation of the transcript (Fig. 4A). In agreement with previous observations (Sheets et al., 1994), the length of the poly(A) tail of CcnB1 increased during oocyte maturation from the germinal-vesicle stage (~50 adenine residues) to the MII stage (~200 adenine residues) (Fig. 4B).

The above RBP depletion experiments indicate that both RBPs are involved in Tex19.1 translation but also show a more profound effect of DAZL than that of CPEB1 on this translation. We have reported that CPEB1 is required for translation of Dazl mRNA and DAZL protein accumulation during oocyte maturation (Chen et al., 2011). Thus, the CPEB1 requirement for Tex19.1 translation might be indirect and entirely dependent on DAZL induction. We then used three complementary approaches to define whether the CPEB1 effects on Tex19.1 are direct. RNA immunoprecipitation was performed with CPEB1-specific antibodies at 0, 5 and 7 h after oocyte entry into prometaphase. The Tex19.1 mRNA, as well as that of other known CPEB1 targets (Dazl and CcnB1), was recovered in the immunoprecipitation pellet of oocyte extracts at the germinal vesicle stage or 5 h after release from meiotic arrest. Conversely, little Tex19.1 mRNA was immunoprecipitated from extracts after 7 h of maturation

(Fig. 5A). This experiment provides a first indication of a physical interaction of CPEB1 with Tex19.1 mRNA. The decreased recovery of Tex19.1 mRNA at 7 h of maturation is consistent with the finding that CPEB1 is degraded during MI after extensive phosphorylation by Cdk1 (Hodgeman et al., 2001; Keady et al., 2007; Setoyama et al., 2007; Chen et al., 2011; Ota et al., 2011); it also confirms the specificity of the immunoprecipitation. Furthermore, we mutated the putative CPEB1-binding CPE in the 3′ UTR of Tex19.1, which had been fused to the luciferase-coding region (Fig. S2A). After microinjection of this construct, we observed that mutation of the CPE significantly decreased translation of the reporter (Fig. 5B). Of note, this latter experimental paradigm excludes the possibility that the effects of CPEB1 are mediated exclusively through an increase in DAZL accumulation. Given the non-consensus nature of the CPE element in Tex19.1, we generated an additional luciferase reporter in which the non-consensus CPE had been mutated to a consensus CPE; this mutation resulted in a fourfold increase in luciferase activity compared to that in wild type (Fig. 5C). These findings confirm the weaker activity of the non-consensus CPE found in the 3′ UTR of Tex19.1.

Activation of translation by DAZL requires multiple DAZL-binding sites

To investigate which DAZL element cooperates with the CPEB for translation, site-directed mutagenesis of the Tex19.1 3′ UTR was used (Fig. S2A,D). On the basis of the consensus (UU[G/C]UU), we mutated the three putative DAZL-binding sites by replacing crucial nucleotides with adenosine. As predicted using the crystal structure of the DAZL RNA recognition motif (RRM) in complex with its target, these mutations should disrupt DAZL binding (Jenkins et al., 2011). This was indeed the case because RIP of FLAG-tagged DAZL showed a progressively reduced ability to bind to the mutant reporter (Fig. 6A). When we used these mutant reporters in a luciferase assay, single mutation of each of these sites caused a decrease in the rate of reporter synthesis (Fig. 6B). Of note, mutation of site 2 (Δ2) was slightly less effective than the other two mutations in decreasing translation at 8 and 16 h. Combined mutation of DAZL sites 1 and 3 (Δ1+3) further decreased the translation of the reporter to minimal levels. Consistent with the results of the luciferase reporter assay, the double mutant was significantly less effective in ribosome loading (Fig. 6C). Thus, the three identified DAZL elements are functional in that they are bound by DAZL and contribute to the overall rate of translation.

CPEB1 and DAZL cooperatively regulate translation of Tex19.1

The double mutant Δ1+3 causes an almost complete loss of translation of the Tex19.1 reporter, suggesting that it also affects the CPEB function. To further investigate the interaction between the function of CPEB1 and DAZL, and given the limited amount of protein available with the oocyte model, we used testes extract, where a large amount of tissue is available, to test the direct interaction between the two RBPs. Immunoprecipitation of CPEB1 led to the recovery of DAZL protein; however, this was abolished upon treatment with ribonuclease A. These results indicate that CPEB1 and DAZL interact with the same RNA targets, but possibly not through a direct interaction between both proteins.

By using an alternative strategy, we assessed whether mutations of the DAZL elements in the 3′ UTR of Tex19.1 affect CPEB1 binding. With this aim, we injected the mutant constructs Δ3 and Δ1+3 into the oocyte. We then used an antibody against CPEB1 for RIP analysis, and the recovery of the luciferase reporter mRNA was measured by using qPCR. A decrease in CPEB1 binding could be detected for both mutants compared to the wild-type reporter (Fig. 7A), suggesting cooperativity at the Tex19.1 3′ UTR.

Because the CPE element present in the 3′ UTR of Tex19.1 is not a consensus element, we used this property to further probe the interaction between DAZL and CPEB1. We reasoned that if a non-consensus CPE is required to generate cooperativity between the two RBPs, mutations to a consensus CPE should affect this synergism. We expressed the 3′ UTR reporter with the mutation generating a consensus CPE in oocytes depleted of DAZL and determined whether translation of the reporter became independent of DAZL. DAZL depletion caused a 72% decrease in luciferase accumulation of the reporter containing the non-consensus CPE, whereas the accumulation of the reporter with the consensus CPE was only marginally affected (29% decrease) (Fig. 7B). This experiment shows that only the non-consensus CPE allows CPEB1 and DAZL to act synergistically.

Multiple DAZL-binding sites are required for the function of DAZL as a translation activator

To investigate whether multiple DAZL and CPE elements are required for translation of other mRNAs present in the oocyte, we re-analyzed the available (Chen et al., 2011) and new polysome array data obtained during oocyte maturation (n=6). The 3′ UTRs of regulated transcripts were scanned for putative CPE and DAZL elements using an algorithm that we had developed previously (Chen et al., 2011). We compared the behavior of transcripts with multiple DAZL elements to that of transcripts without recognizable DAZL elements or transcripts that also possess putative CPEs (Fig. 8). The combined presence of CPE and DAZL elements in transcripts causes a significant shift in the number of transcripts associated with polysomes during maturation (Fig. 8A). Moreover, the combination of non-consensus CPE and DAZL elements produced an even larger shift in the number of transcripts from the repressed to the recruited pool., whereas the presence of a consensus CPE and DAZL elements showed only an increase in the average recruitment of transcripts to the polysomes (Fig. 8B). Thus, cooperativity between non-consensus CPEs and multiple DAZL elements is also detected at a genome-wide level.

DISCUSSION

Meiotic progression and oocyte maturation depends on the translational control of specific stored maternal mRNAs at different stages of the cell cycle. Here, we demonstrate that DAZL functions cooperatively with CPEB1 to regulate translation of maternal mRNAs during mouse oocyte maturation. This cooperative behavior is essential for oocyte meiotic progression because

depletion of either RBP compromises the ability to reach MII. Using candidate and genome-wide approaches, we show that these RBPs cooperate to promote ribosome loading and translation initiation of endogenous mRNA. By using site-directed mutagenesis, we have defined the Tex19.1 cis-regulatory elements that are involved in RBP binding and ribosome loading. Finally, we show that in order for DAZL and CPEB1 synergism to occur, the presence of more than one DAZL-binding element and a non-consensus CPE in the 3′ UTR of mRNAs is required. Thus, translation of a subset of maternal mRNAs is dependent on DAZL acting cooperatively, and possibly sequentially, with CPEB1 during mouse oocyte maturation.

The RiboTag genetic strategy was originally developed to study transcription through the enrichment of cell-type-specific transcripts from a tissue of interest (Sanz et al., 2009, 2013). We have adapted this technique to measure ribosome loading in the oocyte as a surrogate for translation initiation. This approach allows for the isolation of mRNAs that are engaged in translation, providing a temporal snapshot of the maturing oocyte translatome in vivo. We confirmed the power and selectivity of this approach by following the pattern of ribosome loading of at least four distinct maternal mRNAs (Dppa3, Tex19.1, Gdf9 and Paip2). Finally, the RiboTag RIP allows for measurement of candidate transcript in one-tenth the number of oocytes when compared to that required for polysome arrays (Fig. 1C,D), permitting construction of detailed time courses of mRNA translational activation. RiboTag also allowed us to probe the effects of genetic manipulations on maternal mRNA translation by using morpholino-mediated knock down. Of note, because the 60S subunit of the ribosome is tagged, we surmise that recovery of any given transcript in the immunoprecipitated pellet reflects the assembly of a translating ribosome on the mRNA. Even though ribosome stalling could be a confounding factor (Anderson and Kedersha, 2006), in most cases recruitment of the 60S subunit recruitment coincides with the actual initiation of protein synthesis, a step that follows the assembly of the pre-initiation complex (Chew et al., 2013; Dunn et al., 2013). The time course of reporter translation supports this conclusion. Importantly, in the present analysis, we compare the ribosome loading on the same transcript at different stages of maturation or on different genetic backgrounds. When different transcripts are compared, the length of the mRNA and the number of loaded ribosomes might affect recovery during the immunoprecipitation and will require additional corrections or controls.

Binding and functional data provide evidence that Tex19.1 is a target for both DAZL and CPEB1, and that the two RBPs cooperate in the translation of this maternal mRNA during meiosis. DAZL is associated with Tex19.1 in germinal vesicle oocyte extracts, and more so during MII (Chen et al., 2011). Conversely, binding of CPEB1 to the Tex19.1 transcript is detectable in germinal vesicle and prometaphase oocytes but not later in MI or MII, when levels of the CPEB1 protein decrease substantially. This opens the possibility that both proteins are necessary for the initial phase of translation of Tex19.1, whereas DAZL continues to play an important role later in MII when levels of CPEB1 are greatly reduced. A loss-of-function approach could not tease apart these temporal differences, possibly because knock down of the two proteins affects progression to MII, and

because of the fact that accumulation of the DAZL protein is CPEB1 dependent (see below). However, mutagenesis of the DAZL sites in the 3′ UTR suggests that no further translation of the reporter occurs between 8 and 17 h of incubation, suggesting a role later during maturation. CPE mutagenesis does not prevent an increased translation at these late stages of meiotic progression, which is in line with a more prominent function earlier in the cell cycle.

Depletion of CPEB1 causes a 50% decrease in ribosome loading onto the Tex19.1 transcript, whereas DAZL depletion causes a more profound effect (up to 90% reduction). Similar differences were obtained when a luciferase reporter was used in RBP-depleted oocytes or when mutagenesis of the RBPs binding sites was performed. These data strongly suggest that DAZL is required for the CPEB-dependent translation of Tex19.1 mRNA. This requirement is not simply due to the fact that CPEB1 is required for DAZL accumulation in the oocyte (Chen et al., 2011) because DAZL accumulates at a normal level when the CPE mutant construct is used; yet we observe a decrease in translation of the reporter. We propose that CPEB1 binding to the Tex19.1 mRNA and translational activation requires DAZL loading on at least two sites. The non-consensus CPE element is located between two putative DAZL elements. Mutation of the DAZL 1 (Δ1) site decreases binding in a reconstitution system, confirming that it interacts with the DAZL protein. The DAZL site 3 (Δ 3) is instead located 3′ to the CPE site. The crystal structure of CPEB1 suggests that RBPs that bind 3′ to the CPE could be in a favorable position to interact with CPEB1 through the Zn2+-binding domain (ZZ domain). Thus, it is possible that DAZL binding at site 3 might contribute to the stabilization of the CPEB1 binding to a non-consensus site, as suggested by the lower recovery of the Δ3 mutant upon RNA immunoprecipitation with an antibody against CPEB1. Biochemical studies in a heterologous expression system will be required to assess these possibilities. Whether occupancy of DAZL site 1 is possible when the CPEB1 protein is bound to the CPE also remains to be determined experimentally.

An interaction between CPEB1 and DAZL has previously been described in orthologus systems. During Drosophila spermatogenesis, colocalization and a direct interaction has been shown between bol and orb2 (DAZL and CPEB1 fly orthologs, respectively) (Xu et al., 2012). A similar interaction has been reported in immature Xenopus oocytes, where an RNA-independent complex of proteins comprising DAZL, CPEB and CPSF-100 was isolated by using immunoprecipitation (Ota et al., 2011). Because of the limited amount of material available in our study, we could not assess a direct interaction of DAZL with CPEB1 in mouse oocytes. However, an interaction can be inferred by the observation that mutagenesis of the DAZL elements causes a small but significant decrease in CPEB1 binding to a reporter with reduced DAZL-binding ability.

Of note, the DAZL mutant Δ1+3 still contains a DAZL site, yet translation was greatly reduced, suggesting that a single DAZL-binding site is insufficient to stimulate translation. Similarly, removal of a single DAZL site was sufficient to reduce translation significantly, confirming the non-redundant function of these sites. This conclusion is consistent with an earlier observation in a reconstitution

system where forced recruitment of multiple DAZL proteins is necessary to activate translation (Collier et al., 2005).

We show that, like CPEB1, DAZL might also function as a translational repressor in germinal vesicle oocytes. Depletion of either RBP causes a small but significant increase in reporter expression in germinal vesicle oocytes. Such an effect of RBP depletion could not be detected when using other manipulations, such as mutagenesis. This, and the small signal-to-noise ratio, prevented us from further determining the properties of these possible repressive effects. DAZL has been proposed to act as a translational repressor in primordial germ cells (Chen et al., 2015).

Genome-wide analysis has demonstrated a strong correlation between poly(A) tail length and translation in zebrafish and frogs embryos, but not in somatic cells (Subtelny et al., 2014). This conclusion is consistent with data from Xenopus, where it has been shown that cytoplasmic polyadenylation is associated with increased translation. More than a sixfold increase in translation efficiency has been estimated upon a doubling of the poly(A) tail length from 20 to 40 nucleotides (Subtelny et al., 2014). We find a more than threefold increase in the poly(A) tail length of Ccnb1, a known target of CPEB; conversely, a small increase in poly(A) tail length from 150 to 200 residues was measured for Tex19.1 endogenous mRNA. Although this is consistent with other data showing that Tex19.1 is a bona fide CPEB1 target, it is unclear whether this lengthening of the tail is sufficient to signal an increase in translation. Technical hurdles inherent to the experimental system used prevented us from further defining the functional role of these changes in poly(A) tail length.

Our data demonstrate that Tex19.1 is expressed in mouse oocytes, and that translation and protein levels are regulated during oocyte maturation. Both ribosome loading and protein expression show that TEX19.1 progressively accumulates during meiotic progression, with a maximum reached in MII. Tex19.1-null mice have been generated, but the inactivation of this gene in females either produces no phenotype (Tarabay et al., 2013) or decreased fecundity (Ollinger et al., 2008), suggesting that oocyte maturation is not prevented or only marginally affected when Tex19.1 is ablated. Conversely, TEX19.1 plays an essential role during male spermatogenesis as Tex19.1-null males are infertile owing to spermatogenic arrest at meiosis between pachytene and metaphase of MI. It has also been found that Line 1 and intracisternal A-particle (IAP) transposon levels are increased in the Tex19.1-null mice (Ollinger et al., 2008, Tarabay et al., 2013). Spermatogenesis is very sensitive to the activation of endogenous retroviruses, as documented by several knockout models, whereas transposon activation has less of an effect on mammalian oogenesis. Our findings suggest that Tex19.1 accumulation might play a role later, during pre-implantation embryo development.

In summary, we report an adaptation of the RiboTag strategy to investigate the role of RBPs in mammalian oocyte mRNA translation. The above findings demonstrate that DAZL cooperates with CPEB1 in the translational regulation of maternal mRNAs. This regulation is essential for oocyte progression through the

meiotic cell cycle because depletion of either RBP prevents completion of meiosis. DAZL function is required for CPEB1-mediated translational regulation, implying permissive or synergistic effects. This interaction is dependent on the presence of a non-consensus CPE and the presence of multiple DAZL-binding sites on the 3′ UTR of the mRNA. Both CPEB1 and DAZL are expressed and required for germ cell development in the fetal gonad, and we propose that a synergistic interaction between these two proteins plays a key role at other crucial transitions in the life cycle of germ cells (Tay and Richter, 2001; Lin and Page, 2005; Lin et al., 2008).

MATERIALS AND METHODS

Animal husbandry and oocyte collection

Husbandry and experimental procedures involving animal models were approved by the University of California San Francisco Institutional Animal Care and Use Committee. Oocyte collection and in vitro maturation was performed as previously described (Chen et al., 2011). Pure C57Bl6 mice carrying the DAZLTM1Hgu allele (ΔDAZL) were generated as previously described (Chen et al., 2011). Rpl22tm1.1Psam/J (RiboTag) mice, with a targeted mutation that provides conditional expression of the ribosomal protein L22 tagged with three copies of the HA epitope, were developed by Paul S. Amieux (Sanz et al., 2009), and purchased from the Jackson Laboratories. Rpl22tm1.1Psam/J homozygous males were crossed with C57BL/6-TgN(Zp3-cre)82Knw (Jackson Laboratories) females to produce C57BL/6-Zp3cre-Rpl22tm1.1Psam (Zp3cre-RiboTag) mice. C57BL/6-TgN(Zp3-cre)82Knw mice represent a transgenic line where the cre expression is controlled by the regulatory sequences from the mouse zona pellucida 3 (Zp3cre) gene, these were developed by Barbara Knowles (de Vries et al., 2000). C57BL/6-Zp3cre-RiboTag homozygous males were crossed with heterozygous ΔDAZL females to obtain C57BL/6-ΔDAZL-ZP3cre-RiboTag mice.

Immunofluorescence

Immunofluorescence was performed as described previously (Grieshammer et al., 2004). Briefly, ovaries from different genotypes were dissected, fixed in 4% PFA, equilibrated in 30% sucrose and embedded in optimal cutting temperature (OCT) compound. 8-μm cryosections were prepared and subjected to heat-mediated antigen retrieval followed by staining with rabbit anti-VASA (1:400, Abcam, 13840) and mouse anti-HA (1:200, Covance, MMS-101P) antibodies. The following secondary antibodies were used at a dilution of 1:500: donkey anti-mouse IgG conjugated to Alexa-Fluor-594 and donkey anti-rabbit IgG conjugated to Alexa-Fluor-647 from Invitrogen. Confocal imaging was performed using a 20× objective on a Leica SP5 TCS microscope equipped with 405-, 488-, 543-, 594- and 633-nm lasers. Image stacks were analyzed using Volocity (Improvision).

Oocyte culture and microinjections

Oocyte isolation and microinjection was performed in HEPES modified (Sigma-Aldrich, M2645) minimum essential medium Eagle (hMEM; supplemented with 2

μM milrinone). Oocytes were cultured at 37 °C under 5% CO2 in supplemented minimum essential medium α (Gibco, 12561-056) (sMEMα; minimum essential medium α supplemented with 0.2 mM pyruvate, 75 μg/ml penicillin, 10 μg/ml streptomycin sulphate and 3 mg/ml BSA and buffered with 26 mM sodium bicarbonate with or without 2 μM milrinone). Denuded oocytes were injected with 5–10 pl (12.5 ng/μl) of mRNAs using a FemtoJet express programmable microinjector with foot-control-triggered injection (Eppendorf, 5248) and an Automated Upright Microscope System (Leica, DM4000B). Post injection, oocytes were incubated for 3 h in sMEMα containing 2 μM milrinone at 37 °C under 5% CO2.

Oocyte morpholino antisense oligonucleotide microinjections

Germinal vesicle oocytes were isolated in hMEM and incubated for 1 h at 37°C under 5% CO2 in sMEMα with 2 μM milrinone. Then, 5–10 pl of 1 mM morpholino oligonucleotides (Gene Tools) against Dazl (5′ -CCTCAGAAGTTGTGGCAGACATGAT-3′) or Cpeb1 (5′ -CTGCTTCTTCCAGAGAGAAAGCCAT-3′), or a standard control (5′ -CCTCTTACCTCAGTTACAATTTATA-3′) were injected into oocytes using a FemtoJet express microinjector. Post injection, oocytes were incubated overnight in sMEMα containing 2 μM milrinone at 37 °C under 5% CO2 before in vitro maturation in sMEMα without milrinone.

Reporter mRNA preparation and luciferase assay

The injection control reporter pCDNA3-Firefly-Luc (FFL) and the Renilla luciferase reporter (RL), with the 3′ UTR of mouse Tex19.1 (pRL-TK-Tex19.1+3′ UTR) cloned into the pRL-TK vector (Promega, E2241), have been previously described (Chen et al., 2011). Point mutations in pRL-TK-Tex19.1+3′ UTR to ablate the putative binding sites of DAZL and CPEB1 were cloned using the QuikChange II XL Site-Directed Mutagenesis kit (Agilent Technologies, 200521). Luciferase reporters were transcribed in vitro to synthesize mRNAs using the mMESSAGE mMACHINE T7® kit (Ambion, AM1344). The injection control Firefly luciferase mRNA was polyadenylated with the Poly(A) tailing kit (Ambion, AM1350). Luciferase activity was assessed with the Dual Luciferase Reporter Assay kit (Promega, E1910) and detected with the SpectraMaxL Luminometer (Molecular Devices). Data are reported as the ratios of the luminescence of the Renilla luciferase reporter to that of Firefly luciferase.

HEK293T cell culture and transfection

HEK293T cells were maintained at 37°C under 5% CO2 in Dulbecco's modified Eagle medium (Gibco, 1960-044) supplemented with 4 mM l-glutamine (Gibco, 25030-081) and 10% fetal bovine serum (Gibco, 16000-044). Cells were grown to 70% confluence and incubated with transfection mix (for DNA, Lipofectamine LTX® Reagent (Invitrogen, 15338030) complexes in Opti-MEM I reduced-serum medium without serum (Gibco, 31985070) for 24 h. Cells were washed in ice-cold PBS and collected in PLB [15 mM Tris-HCl pH 7.5, 50 mM NaCl, 5 mM MgCl2,

1% Triton, 0.15 mM Na3VO4, 10 mM β-glycerophosphate, 1 mM DTT (Sigma-Aldrich, 646563), protease inhibitors (Sigma-Aldrich, P8340), 40 U RNase OUT (Invitrogen, 10777-019), 100 µg/ml cycloheximide (Sigma-Aldrich, C7698) and 2 mM vanadyl ribonucleoside (NEB, S1402S)].

Immunoprecipitation

RiboTag samples
Oocytes were collected, washed in RNase-free PBS with 1% polyvinylpyrrolidone and transferred to 300 µl of supplemented homogenization buffer [S-HB; 50 mM Tris-HCl pH 7.4, 100 mM KCl, 12 mM MgCl2, 1% NP-40, 1 mM dithiothreitol, protease inhibitors, 40 U RNAseOUT, 100 µg/ml cycloheximide and 1 mg/ml heparin (Sigma-Aldrich, H3393)]. Then, 3 µg of anti-HA antibody (Covance, MMS-101R) or mouse IgG (Abcam, ab37355) was added to the oocyte lysate and incubated for 4 h at 4°C on a rotor. 25 µl of pre-washed protein G magnetic Dynabeads (Invitrogen, 10007D) were added to each lysate and incubated for 5 h at 4°C on a rotor. Beads were washed with high-salt buffer five times (50 mM Tris-HCl pH 7.4, 300 mM KCl, 12 mM MgCl2, 1% NP-40, 1 mM dithiothreitol, 40 U RNAseOUT and 100 µg/ml cycloheximide). RNA was eluted from beads with 200 µl of supplemented RTL lysis buffer (Qiagen, 74034). RNA extraction was performed using the RNeasy Micro Plus kit according to manufacturer's instructions. Extracted RNA was used to prepare cDNA using the SuperScript III First-Strand Synthesis system (Invitrogen, 18080-051) using random hexamer oligonucleotide primers.

mRNA–protein complexes
RIP analysis was performed as described previously (Chen et al., 2011). Briefly, 200 oocytes were lysed using PLB. Lysate was pre-cleared with pre-washed protein-G–Sepharose beads (Invitrogen, P3296) for 1 h at 4°C. Pre-cleared lysates were incubated with a specific antibody or the corresponding IgG control for 5 h at 4°C on a rotor. Beads were washed with PLB for 5 min five times. RNA was extracted and purified with the RNeasy Plus Micro kit, and cDNA was prepared with the SuperScript III First-Strand Synthesis system using random hexamer oligonucleotide primers. The antibody against CPEB1 was from Abcam (catalog number ab73287, lot GR142423).

Western blot

Oocytes were extracted in Laemmli buffer (Bio-Rad) supplemented with mercaptoethanol, and a cocktail of phosphatase and protease inhibitors (Roche). The extracts were boiled and separated on 8% polyacrylamide gels and transferred to a PVDF membrane. TEX19.1 was immunolabeled by incubating the membrane with a solution of anti-TEX19.1 antibody (1:500) (Tarabay et al., 2013). An antibody against α-tubulin (T6074, Sigma-Aldrich; 1:10,000) was used as loading control.

Real-time qPCR

Real-time qPCR was performed using KAPA SYBR FAST ABI Prism 2× qPCR master mix (Kapa Biosystems, KK4603) in an ABI 7900 Real-Time PCR system (Applied Biosystems). Oligonucleotide primer pairs were designed against two exons flanking an intron. Primer specificity was verified by using dissociation curve analysis, performed at the end of the amplification. Fold-enrichment was calculated using the 2−ΔΔCt method (Livak and Schmittgen, 2001).

Poly(A) tail length assay

Total RNA was extracted from 100 oocytes using the RNeasy Micro Plus kit. The total volume of RNA extracted was used in the Poly(A) tail length assay using the Poly(A) Tail Length Assay kit (Affymetrix, 76455). Poly(A) size was determined by subtracting the PCR amplicon size obtained with the 'Universal primer' from that of the transcript-specific primer.

Statistical analysis

Statistical analysis was performed using the Prism 5.01 GraphPad package. The statistical analysis performed depended on specific experiments and is described within the figure legend. Statistical significance is denoted as *P<0.05, **P<0.01, ***P<0.001, ****P<0.0001 and 'ns' for not statistically significant.

Acknowledgements

The authors are indebted to Stanley McKnight and Paul Amieux (University of Washington, Seattle, WA) for helpful discussion during the optimization of the RiboTag strategy for oocytes, and to Qiaohong Zhao for performing the genotyping of the mice.

Competing interests

The authors declare no competing or financial interests.

Author contributions

J.P.S.M. and M.C. designed experiments, analyzed data and wrote the manuscript. J.P.S.M. performed all the experiments with the help of X.L. in animal handling and oocyte collection, F.F. for one of the mutant microinjection experiments, and R.A. and D.J.L. in imaging protein expression. Bioinformatic analysis was performed by A.O., J.C.F. and M.C. S.F. provided reagents and advice on Tex19.1 physiological function.

Funding

This work was supported by the National Institutes of Health [grant number RO1-GM097165]; and the Eunice Kennedy Shriver National Institute of Child Health and Human Development and NIH cooperative agreement [grant number P50HD055764] as part of the Specialized Cooperative Centers Program in Reproduction and Infertility Research (to M.C.). F.F. is supported by the FP7

project [grant numbers FP7-PEOPLE-2013-IOF GA and 624874 MateRNA]. Deposited in PMC for release after 12 months.

Supplementary information

Supplementary information available online at
http://jcs.biologists.org/lookup/suppl/doi:10.1242/jcs.179218/-/DC1

References

1. Anderson P. and Kedersha N. (2006). RNA granules. J. Cell Biol. 172, 803-808. 10.1083/jcb.200512082
2. Brook M., Smith J. W. S. and Gray N. K. (2009). The DAZL and PABP families: RNA-binding proteins with interrelated roles in translational control in oocytes. Reproduction 137, 595-617. 10.1530/REP-08-0524 [
3. Brower P. T., Gizang E., Boreen S. M. and Schultz R. M. (1981). Biochemical studies of mammalian oogenesis: synthesis and stability of various classes of RNA during growth of the mouse oocyte in vitro. Dev. Biol. 86, 373-383. 10.1016/0012-1606(81)90195-0
4. Cao Q. and Richter J. D. (2002). Dissolution of the maskin-eIF4E complex by cytoplasmic polyadenylation and poly(A)-binding protein controls cyclin B1 mRNA translation and oocyte maturation. EMBO J. 21, 3852-3862. 10.1093/emboj/cdf353
5. Chen J., Melton C., Suh N., Oh J. S., Horner K., Xie F., Sette C., Blelloch R. and Conti M. (2011). Genome-wide analysis of translation reveals a critical role for deleted in azoospermia-like (Dazl) at the oocyte-to-zygote transition. Genes Dev. 25, 755-766. 10.1101/gad.2028911
6. Chen H.-H., Welling M., Bloch D. B., Muñoz J., Mientjes E., Chen X., Tramp C., Wu J., Yabuuchi A., Chou Y.-F. et al. (2015). DAZL limits pluripotency, differentiation, and apoptosis in developing primordial germ cells. Stem Cell Rep. 3, 892-904. 10.1016/j.stemcr.2014.09.003
7. Chew G.-L., Pauli A., Rinn J. L., Regev A., Schier A. F. and Valen E. (2013). Ribosome profiling reveals resemblance between long non-coding RNAs and 5′ leaders of coding RNAs. Development 140, 2828-2834. 10.1242/dev.098343
8. Clarke H. J. (2012). Post-transcriptional control of gene expression during mouse oogenesis. Results Probl. Cell Differ. 55, 1-21. 10.1007/978-3-642-30406-4_1
9. Collier B., Gorgoni B., Loveridge C., Cooke H. J. and Gray N. K. (2005). The DAZL family proteins are PABP-binding proteins that regulate translation in germ cells. EMBO J. 24, 2656-2666. 10.1038/sj.emboj.7600738
10. de Vries W. N., Binns L. T., Fancher K. S., Dean J., Moore R., Kemler R. and Knowles B. B. (2000). Expression of Cre recombinase in mouse oocytes: a means to study maternal effect genes. Genesis 26, 110-112. 10.1002/(SICI)1526-968X(200002)26:2<110::AID-GENE2>3.0.CO;2-8
11. Dunn J. G., Foo C. K., Belletier N. G., Gavis E. R. and Weissman J. S. (2013). Ribosome profiling reveals pervasive and regulated stop codon readthrough in Drosophila melanogaster. Elife 2, e01179 10.7554/eLife.01179

12. Fernandez-Miranda G. and Mendez R. (2012). The CPEB-family of proteins, translational control in senescence and cancer. Ageing Res. Rev. 11, 460-472. 10.1016/j.arr.2012.03.004
13. Gosden R. and Lee B. (2010). Portrait of an oocyte: our obscure origin. J. Clin. Invest. 120, 973-983. 10.1172/JCI41294
14. Grieshammer U., Le M. U., Plump A. S., Wang F., Tessier-Lavigne M. and Martin G. R. (2004). SLIT2-mediated ROBO2 signaling restricts kidney induction to a single site. Dev. Cell 6, 709-717. 10.1016/S1534-5807(04)00108-X
15. Hake L. E. and Richter J. D. (1994). CPEB is a specificity factor that mediates cytoplasmic polyadenylation during Xenopus oocyte maturation. Cell 79, 617-627. 10.1016/0092-8674(94)90547-9
16. Hamatani T., Carter M. G., Sharov A. A. and Ko M. S. H. (2004). Dynamics of global gene expression changes during mouse preimplantation development. Dev. Cell 6, 117-131. 10.1016/S1534-5807(03)00373-3
17. Hodgeman R., Tay J., Mendez R. and Richter J. D. (2001). CPEB phosphorylation and cytoplasmic polyadenylation are catalyzed by the kinase IAK1/Eg2 in maturing mouse oocytes. Development 128, 2815-2822.
18. Jenkins H. T., Malkova B. and Edwards T. A. (2011). Kinked beta-strands mediate high-affinity recognition of mRNA targets by the germ-cell regulator DAZL. Proc. Natl. Acad. Sci. USA 108, 18266-18271. 10.1073/pnas.1105211108
19. Keady B. T., Kuo P., Martinez S. E., Yuan L. and Hake L. E. (2007). MAPK interacts with XGef and is required for CPEB activation during meiosis in Xenopus oocytes. J. Cell Sci. 120, 1093-1103. 10.1242/jcs.03416
20. Kim J. H. and Richter J. D. (2006). Opposing polymerase-deadenylase activities regulate cytoplasmic polyadenylation. Mol. Cell 24, 173-183. 10.1016/j.molcel.2006.08.016
21. Kim J. H. and Richter J. D. (2007). RINGO/cdk1 and CPEB mediate poly(A) tail stabilization and translational regulation by ePAB. Genes Dev. 21, 2571-2579. 10.1101/gad.1593007
22. Lin Y. and Page D. C. (2005). Dazl deficiency leads to embryonic arrest of germ cell development in XY C57BL/6 mice. Dev. Biol. 288, 309-316. 10.1016/j.ydbio.2005.06.032
23. Lin Y., Gill M. E., Koubova J. and Page D. C. (2008). Germ cell-intrinsic and -extrinsic factors govern meiotic initiation in mouse embryos. Science 322, 1685-1687. 10.1126/science.1166340
24. Livak K. J. and Schmittgen T. D. (2001). Analysis of relative gene expression data using real-time quantitative PCR and the 2(-Delta Delta C(T)) Method. Methods 25, 402-408. 10.1006/meth.2001.1262
25. McGrew L. L. and Richter J. D. (1990). Translational control by cytoplasmic polyadenylation during Xenopus oocyte maturation: characterization of cis and trans elements and regulation by cyclin/MPF. EMBO J. 9, 3743-3751.
26. Ollinger R., Childs A. J., Burgess H. M., Speed R. M., Lundegaard P. R., Reynolds N., Gray N. K., Cooke H. J. and Adams I. R. (2008). Deletion of the pluripotency-associated Tex19.1 gene causes activation of endogenous

retroviruses and defective spermatogenesis in mice. PLoS Genet. 4, e1000199 10.1371/journal.pgen.1000199
27. Ota R., Kotani T. and Yamashita M. (2011). Biochemical characterization of Pumilio1 and Pumilio2 in Xenopus oocytes. J. Biol. Chem. 286, 2853-2863. 10.1074/jbc.M110.155523
28. Pique M., Lopez J. M., Foissac S., Guigo R. and Mendez R. (2008). A combinatorial code for CPE-mediated translational control. Cell 132, 434-448. 10.1016/j.cell.2007.12.038
29. Radford H. E., Meijer H. A. and de Moor C. H. (2008). Translational control by cytoplasmic polyadenylation in Xenopus oocytes. Biochim. Biophys. Acta 1779, 217-229. 10.1016/j.bbagrm.2008.02.002
30. Reichmann J., Reddington J. P., Best D., Read D., Ollinger R., Meehan R. R. and Adams I. R. (2013). The genome-defence gene Tex19.1 suppresses LINE-1 retrotransposons in the placenta and prevents intra-uterine growth retardation in mice. Hum. Mol. Genet. 22, 1791-1806. 10.1093/hmg/ddt029
31. Reynolds N., Collier B., Maratou K., Bingham V., Speed R. M., Taggart M., Semple C. A., Gray N. K. and Cooke H. J. (2005). Dazl binds in vivo to specific transcripts and can regulate the pre-meiotic translation of Mvh in germ cells. Hum. Mol. Genet. 14, 3899-3909. 10.1093/hmg/ddi414
32. Reynolds N., Collier B., Bingham V., Gray N. K. and Cooke H. J. (2007). Translation of the synaptonemal complex component Sycp3 is enhanced in vivo by the germ cell specific regulator Dazl. RNA 13, 974-981. 10.1261/rna.465507
33. Ruggiu M., Speed R., Taggart M., McKay S. J., Kilanowski F., Saunders P., Dorin J. and Cooke H. J. (1997). The mouse Dazla gene encodes a cytoplasmic protein essential for gametogenesis. Nature 389, 73-77. 10.1038/37987
34. Sanz E., Yang L., Su T., Morris D. R., McKnight G. S. and Amieux P. S. (2009). Cell-type-specific isolation of ribosome-associated mRNA from complex tissues. Proc. Natl. Acad. Sci. USA 106, 13939-13944. 10.1073/pnas.0907143106
35. Sanz E., Evanoff R., Quintana A., Evans E., Miller J. A., Ko C., Amieux P. S., Griswold M. D. and McKnight G. S. (2013). RiboTag analysis of actively translated mRNAs in Sertoli and Leydig cells in vivo. PLoS ONE 8, e66179 10.1371/journal.pone.0066179
36. Saunders P. T., Turner J. M., Ruggiu M., Taggart M., Burgoyne P. S., Elliott D. and Cooke H. J. (2003). Absence of mDazl produces a final block on germ cell development at meiosis. Reproduction 126, 589-597. 10.1530/rep.0.1260589
37. Setoyama D., Yamashita M. and Sagata N. (2007). Mechanism of degradation of CPEB during Xenopus oocyte maturation. Proc. Natl. Acad. Sci. USA 104, 18001-18006. 10.1073/pnas.0706952104 [
38. Sheets M. D., Fox C. A., Hunt T., Vande Woude G. and Wickens M. (1994). The 3′-untranslated regions of c-mos and cyclin mRNAs stimulate translation by regulating cytoplasmic polyadenylation. Genes Dev. 8, 926-938. 10.1101/gad.8.8.926

39. Subtelny A. O., Eichhorn S. W., Chen G. R., Sive H. and Bartel D. P. (2014). Poly(A)-tail profiling reveals an embryonic switch in translational control. Nature 508, 66-71. 10.1038/nature13007
40. Takeda Y., Mishima Y., Fujiwara T., Sakamoto H. and Inoue K. (2009). DAZL relieves miRNA-mediated repression of germline mRNAs by controlling poly(A) tail length in zebrafish. PLoS ONE 4, e7513 10.1371/journal.pone.0007513
41. Tarabay Y., Kieffer E., Teletin M., Celebi C., Van Montfoort A., Zamudio N., Achour M., El Ramy R., Gazdag E., Tropel P. et al. (2013). The mammalian-specific Tex19.1 gene plays an essential role in spermatogenesis and placenta-supported development. Hum. Reprod. 28, 2201-2214. 10.1093/humrep/det129
42. Tay J. and Richter J. D. (2001). Germ cell differentiation and synaptonemal complex formation are disrupted in CPEB knockout mice. Dev. Cell 1, 201-213. 10.1016/S1534-5807(01)00025-9
43. Xu S., Hafer N., Agunwamba B. and Schedl P. (2012). The CPEB protein Orb2 has multiple functions during spermatogenesis in Drosophila melanogaster. PLoS Genet. 8, e1003079 10.1371/journal.pgen.1003079

Figure Legends

Fig. 1.

Immunoprecipitation of ribosome-associated maternal mRNAs predicts translation. (A,B) Expression of the HA tag in oocytes. Ovaries expressing the RiboTag under the control of the Zp3 promoter (Zp3-RiboTag; A) or the control construct (B) were stained for HA and VASA (also known as DDX4). Scale bars: 50 μm (A); 200 μm (B). (C) Polysome array signals of transcripts representative of the three different classes of mRNAs during oocyte maturation. Gdf9 (class I, constitutively expressed), Paip2 (class II, repressed) and Tex19.1 (class III, activated). Mean±s.e.m., n=3 independent biological replicates. (D) qPCR analysis of mRNAs recovered using RiboTag RIP for the three transcripts reported in C. Data are expressed as a ratio between the qPCR signal from immunoprecipitations from control (WT) and Zp3-RiboTag oocytes. Mean±range of two independent experiments. (E) Time course of RiboTag RIP of Tex19.1 and Dppa3 during oocyte maturation. Fold enrichment was calculated as $2-\Delta\Delta CT$ over the nonspecific (NS) control IgG. Data were normalized against input values. Mean±s.e.m. (n=5 independent experiments and 3 for the controls). (F) Expression of a luciferase reporter under the control of the Tex19.1 3′ UTR throughout oocyte maturation. The reporter luciferase signal (Renilla luciferase, RLuc) was normalized to that of the firefly luciferase (FFLuc) injection control. Mean±s.e.m., n=15 independent experiments. Inset shows immunodetection of TEX19.1 protein during oocyte maturation; the bar graph represents the average intensity±s.e.m. of three different biological replicates. GV, germinal vesicle; GVBD, germinal vesicle breakdown; MI, metaphase of meiosis I; MII, metaphase of meiosis II; TUB, tubulin.

Fig. 2.

Ribosome loading onto Tex19.1 is under CPEB1 and DAZL control. (A) Knockdown of CPEB1 in mouse oocytes decreases ribosome recruitment onto Tex19.1 and CcnB1 mRNAs. Germinal vesicle Zp3-RiboTag oocytes were injected

with a morpholino against Cpeb1 (CPEB1-MO), or a control MO (Ctr MO), incubated overnight, matured for 5 h and then analyzed using RiboTag RIP. qPCR analysis was performed for Tex19.1, CcnB1 and Rpl19 as a control. (B) Knockdown of DAZL significantly reduced ribosome loading onto Tex19.1 but showed no effect in CcnB1 or Rpl19 levels. DAZL+/−-Zp3-RiboTag (heterozygous, Het) and DAZL+/+-Zp3-RiboTag (wild type, WT) oocytes were injected with control or DAZL-MO. RiboTag RIP precipitates from oocytes collected at 5-h post meiotic re-entry were used for qPCR analysis for Tex19.1, CcnB1 and Rpl19. Fold enrichment in A and B was calculated as 2−ΔΔCT against the RNAs from RIP using the non-specific IgG control and normalized against input values. *P<0.05, **P<0.01, ***P<0.001 (two-tailed paired t-test). The data are reported as individual experiments (circles) or as mean±s.e.m. of three or four independent experiments (bars).

Fig. 3.
Translation of the Tex19.1 reporter requires both CPEB1 and DAZL. Germinal vesicle oocytes were co-injected with RBP-specific MOs (CPEB1, A; DAZL, B) or control MO (Cont MO), and a luciferase reporter with the 3′ UTR of Tex19.1. After release from the germinal vesicle stage, injected oocytes were collected at different times of maturation, and luciferase activity was measured. Significance was assessed by using two-way ANOVA with Bonferroni correction comparing the reporter accumulation in MO-knockdown and control MO-injected oocytes. (C,D) Time 0 of oocyte maturation from the time courses shown in A and B of groups injected with control MO and MOs specific to each of the two RBPs. Significance was determined by a two-tailed paired t-test. Renilla Luciferase (RLuc) units were normalized to firefly luciferase (FFLuc) activity injected as a control. Each point is the mean±s.e.m. of five or six independent pools of injected oocytes. *P<0.05; ***P<0.001; ns, not statistically significant.

Fig. 4.
Meiotic re-entry is dependent on cytoplasmic polyadenylation. (A) Tex19.1 is polyadenylated upon meiotic re-entry. PAT assay of Tex19.1 from mouse oocytes at different stages of maturation. n=6 independent experiments. (B) CcnB1 is polyadenylated upon meiotic re-entry. PAT assay of CcnB1 from mouse oocytes at different stages of maturation. The experiment was repeated three times, and the mean and range is reported. GV, germinal vesicle; MI, metaphase of meiosis I; MII, metaphase of meiosis II; bp, base pairs. Average±range of three independent experiments. **P<0.01; ns, not statistically significant (one-way ANOVA).

Fig. 5.
CPEB1 has a direct effect on Tex19.1 translation. (A) CPEB1 is bound to Tex19.1. Oocytes were matured in vitro and used for a RIP with CPEB1; qPCR analysis was performed on the immunoprecipitated pellets. Fold enrichment was calculated as 2−ΔΔCT against the RNAs from RIP with the non-specific IgG control. Data are represented as mean±s.e.m. of three independent experiments, or reporting biological replicates as individual points. (B,C) Germinal vesicle (GV) oocytes were injected with a luciferase reporter containing the wild-type 3′ UTR of Tex19.1 with a non-consensus CPE (WT-ncCPE) or a mutated CPE (ΔCPE; B), or with a mutant 3′ UTR modified to a consensus CPE (cCPE; C) and

matured in vitro. Luciferase activity was measured between times 0 and 17 h of oocyte maturation. ****P<0.0001; ns, not statistically significant. Significance was assessed with a two-way ANOVA with Bonferroni correction comparing the progression of the WT-ncCPE with the mutated reporters (cCPE or ΔCPE) during oocyte maturation.

Fig. 6.
DAZL regulates translation of Tex19.1. (A) Multiple DAZL proteins bind to the Tex19.1 3′ UTR simultaneously. HEK293T cells were co-transfected with DAZL–Flag and one of three Tex19.1 luciferase reporters [wild type (WT), mutant of site 1 (Δ1) and mutant of site 2 (Δ 2)]. qPCR analysis for Renilla luciferase was performed on the FLAG RIP (α -FLAG) samples. FLAG RIP data were normalized to the negative control IgG RIP. (B) Germinal vesicle oocytes were injected with a luciferase reporter with the 3′ UTR of Tex19.1 containing three putative DAZL-binding sites, or reporters with mutations in the putative DAZL-binding sites. The reporter luciferase signal (Renilla Luciferase, RLuc) was normalized to the firefly luciferase (FFLuc) injection control. (C) Deletion of putative DAZL-binding sites caused a decrease in ribosome loading into a Tex19.1 reporter. Zp3-RiboTag-expressing oocytes were injected with a luciferase reporter containing the endogenous 3′ UTR of Tex19.1 or a reporter with two putative DAZL-binding sites mutated (Δ1+3); oocytes were then matured for 5 h. A RiboTag RIP was performed followed by qPCR analysis for Renilla luciferase. Fold enrichment was calculated as 2−ΔΔCT against those RNAs from RIP with the non-specific IgG control. Data are reported as mean±s.e.m., and independent biological replicates are also reported as single points. Statistical significances for A and C were calculated with a two-tailed paired t-test, and for B by a two-way ANOVA with Bonferroni correction comparing the progression of the wild type to the mutated reporters during oocyte maturation. *P<0.05; **P<0.01; ***P<0.001; ****P<0.0001; ns, not statistically significant.

Fig. 7.
Synergistic effect between CPEB1 and DAZL. (A) Deletion of one or two DAZL-binding sites (Δ3 or Δ1+3) results in a decrease in CPEB1 binding to a common mRNA target. RIP was performed in germinal vesicle oocytes, followed by a qPCR analysis for Renilla luciferase. Fold enrichment was calculated as 2−ΔΔCT against those RNAs from RIP with the non-specific IgG control; data are expressed as percentages of the results obtained using the wild-type Tex19.1 3' UTR (WT). Data are reported as mean±s.e.m. with individual points representing each biological replicate. (B) The properties of the CPE determines the effect of DAZL on translation. Oocytes were co-injected with a control MO or a Dazl MO, and a Tex19.1 reporter construct with the endogenous CPE (WT) or a CPE mutated to consensus (cCPE). At the times indicated in the abscissa, oocytes were harvested and luciferase activity measured. Each bar represents the mean±s.e.m. of six to eight independent experiments. **P<0.01 (two-tailed paired t-test). IP, immunoprecipitation.

Fig. 8.
Bioinformatic analysis of the relationship between the number of DAZL-binding and CPE elements and the recruitment of oocyte transcripts to the polysomes.

(A) Computational analysis of the polysome array dataset for CPE and DAZL-binding site interactions. The 3′ UTRs of all the present transcripts were scanned for CPE or DAZL-binding putative sites. Transcripts were then subdivided into groups according to the presence and number of putative elements. Samples were binned according to the Log2 fold-change in polysome loading during maturation as derived from the array. Note the progressive shift to the right of transcripts containing DAZL-binding and CPE sites. (B) The cumulative fold-change for transcripts containing no DAZL-binding sites (No Dazl) or one (1 Dazl) or more (>1 Dazl) DAZL-binding elements was related to the presence of non-consensus or consensus CPEs.

Figure 1

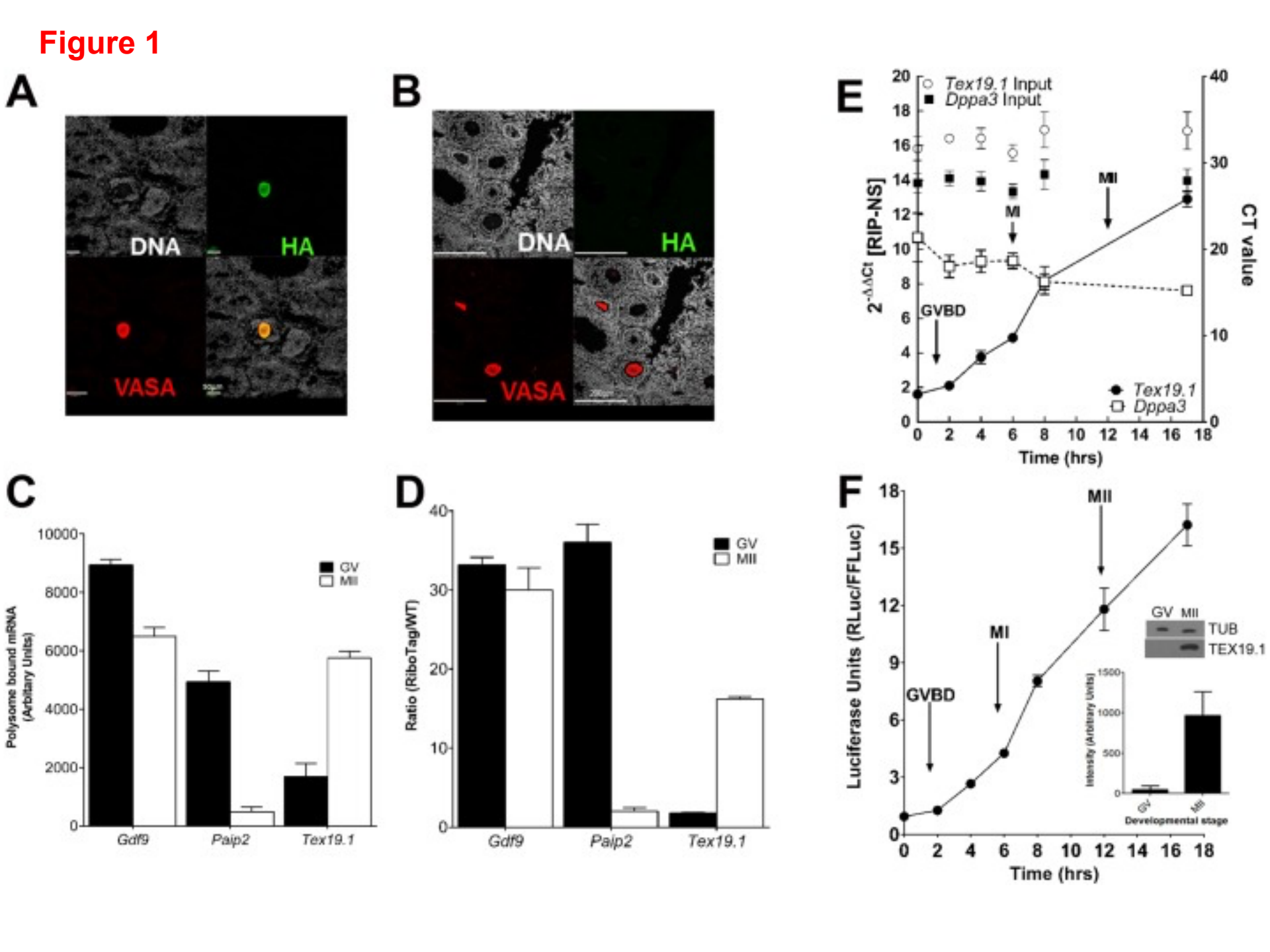
A
DNA
HA
VASA
B
DNA
HA
VASA
C
Polysome bound mRNA (Arbitary Units)
GV
MII
Gdf9
Paip2
Tex19.1
D
Ratio (RiboTag/WT)
GV
MII
Gdf9
Paip2
Tex19.1
E
Tex19.1 Input
Dppa3 Input
2^-ΔΔCt [RIP-NS]
CT value
GVBD
MI
MII
Tex19.1
Dppa3
Time (hrs)
F
Luciferase Units (RLuc/FFLuc)
GVBD
MI
MII
GV MII
TUB
TEX19.1
Intensity (Arbitrary Units)
Developmental stage
Time (hrs)

Figure 2

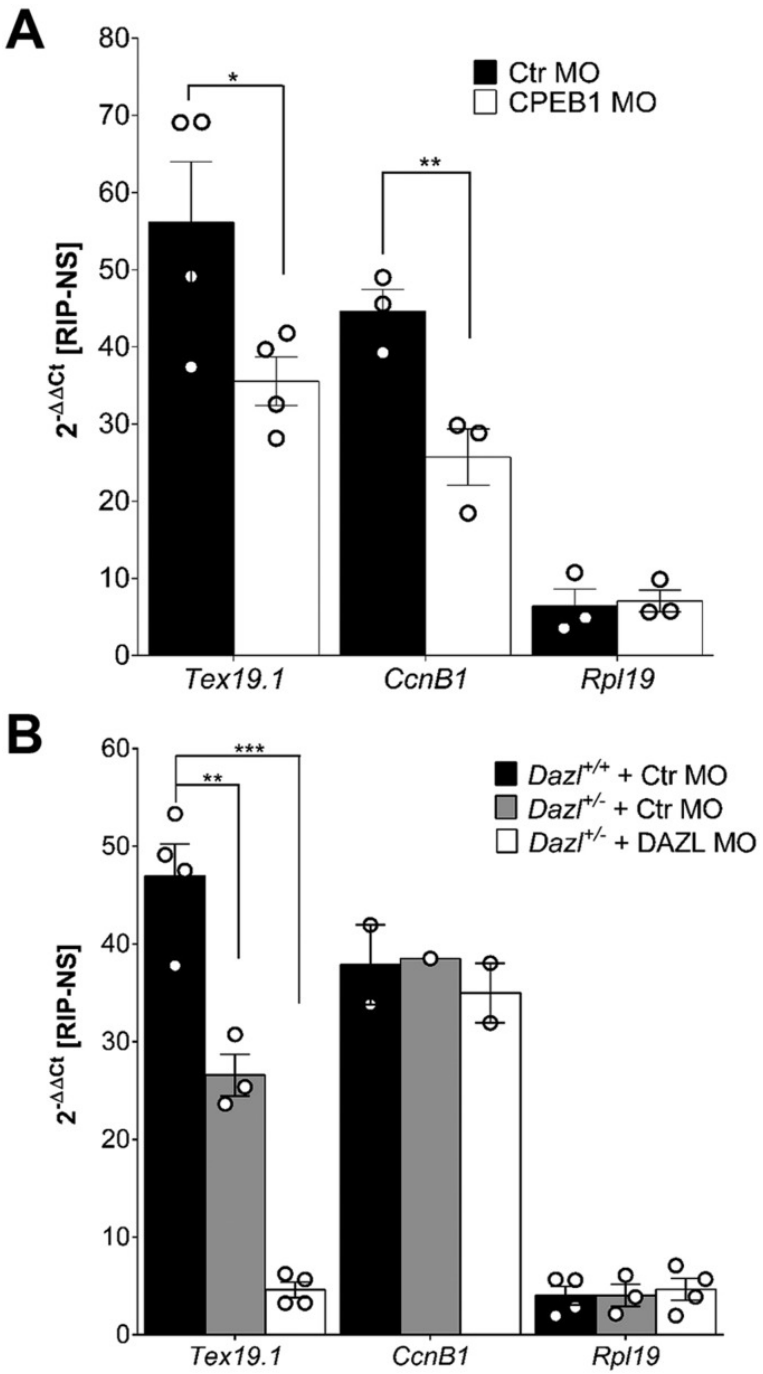
A
Ctr MO
CPEB1 MO
2-ΔΔCt [RIP-NS]
80
70
60
50
40
30
20
10
0
*
**
Tex19.1
CcnB1
Rpl19
B
Dazl+/+ + Ctr MO
Dazl+/- + Ctr MO
Dazl+/- + DAZL MO
2-ΔΔCt [RIP-NS]
60
50
40
30
20
10
0
***
**
Tex19.1
CcnB1
Rpl19

Figure 3

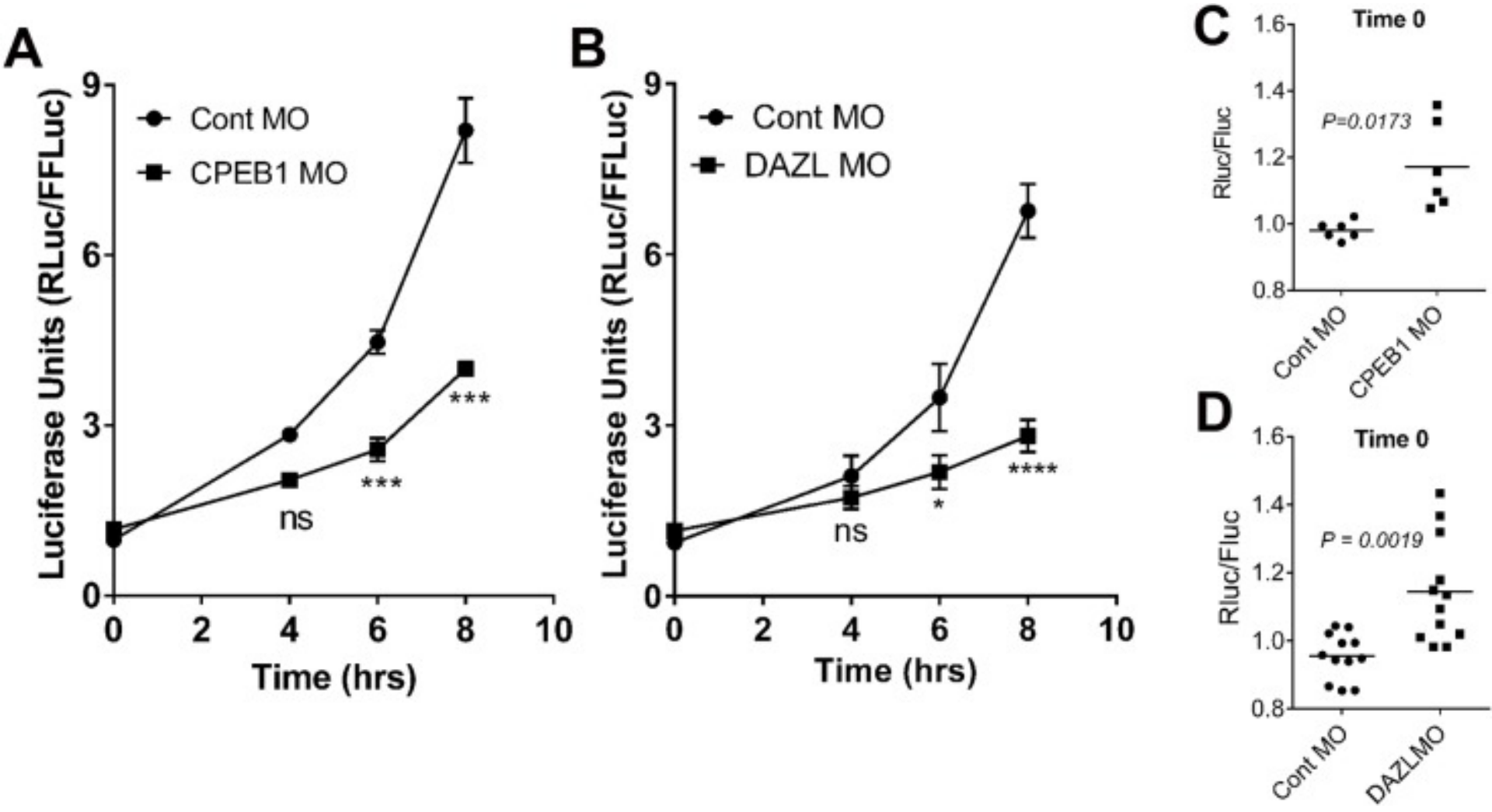
A
Cont MO
CPEB1 MO
Luciferase Units (RLuc/FFLuc)
Time (hrs)
ns
***
***
B
Cont MO
DAZL MO
Luciferase Units (RLuc/FFLuc)
Time (hrs)
ns
*
****
C
Time 0
Rluc/Fluc
P=0.0173
Cont MO
CPEB1 MO
D
Time 0
Rluc/Fluc
P = 0.0019
Cont MO
DAZLMO

Figure 4

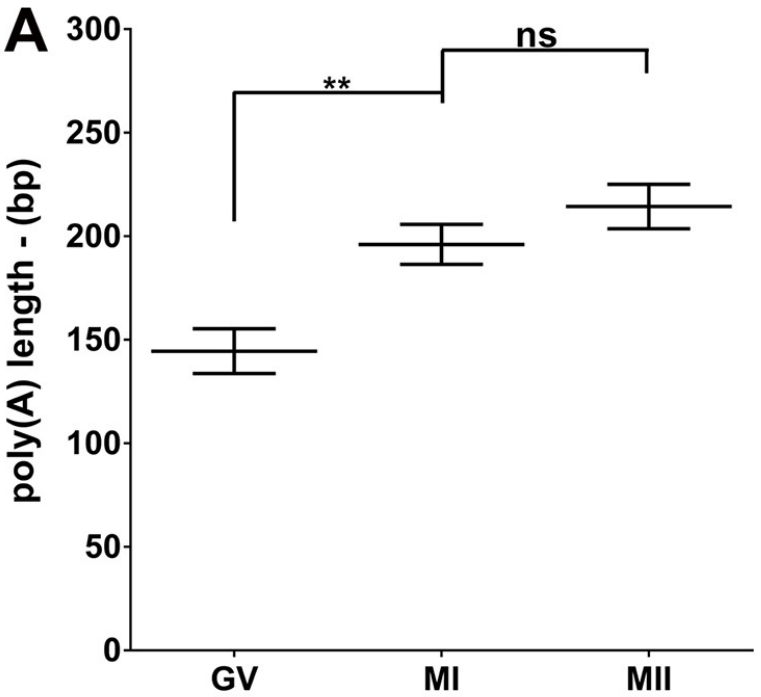
A
300
250
200
150
100
50
0
poly(A) length - (bp)
**
ns
GV
MI
MII

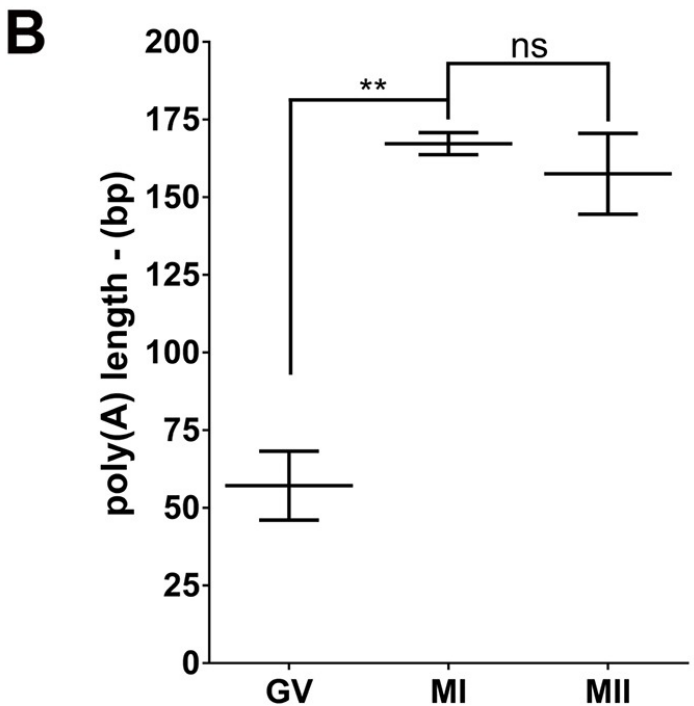
B
200
175
150
125
100
75
50
25
0
poly(A) length - (bp)
**
ns
GV
MI
MII

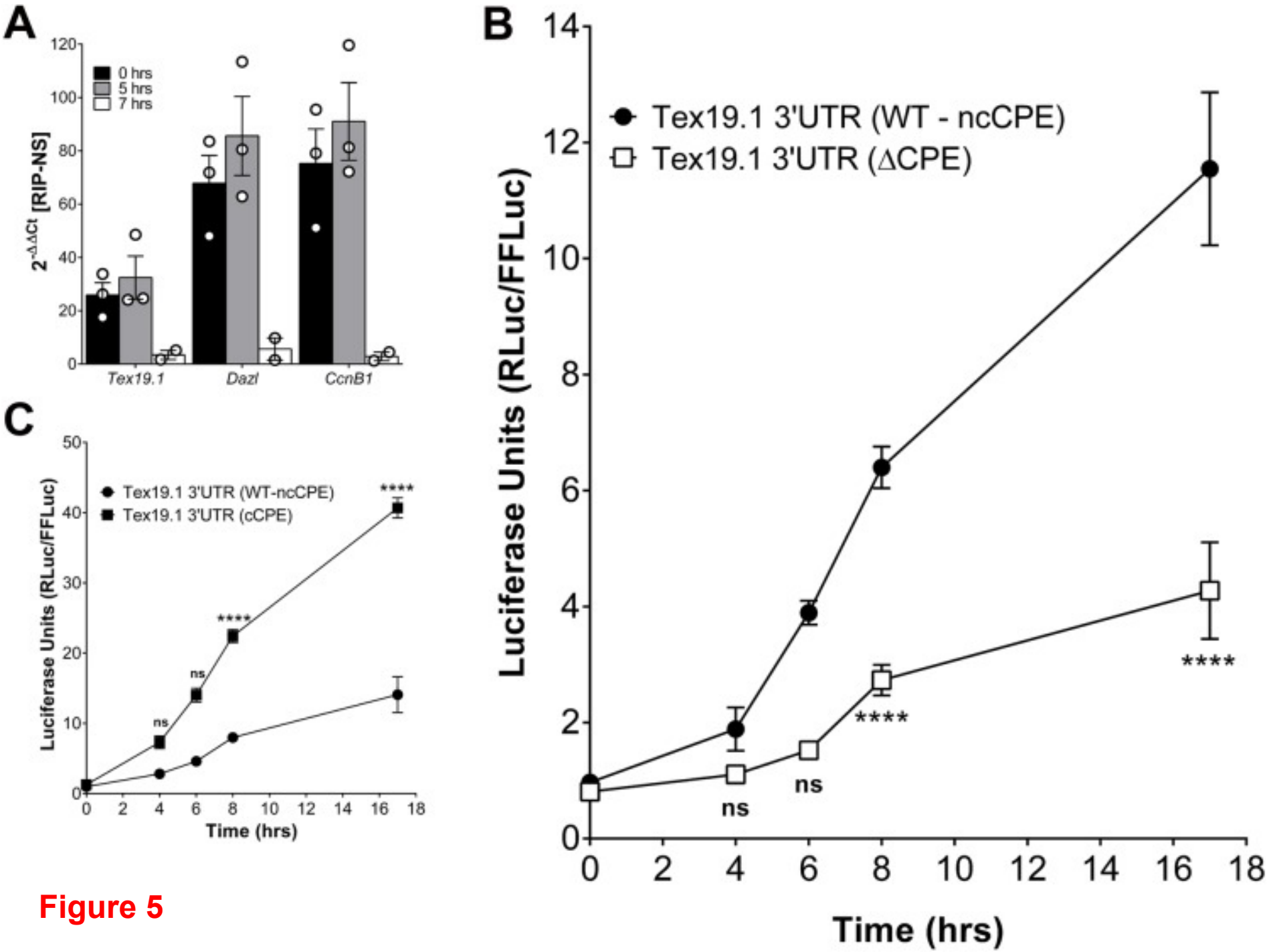
A
120
100
80
60
40
20
0
0 hrs
5 hrs
7 hrs
2-ΔΔCt [RIP-NS]
Tex19.1
Dazl
CcnB1
B
14
12
10
8
6
4
2
0
Tex19.1 3'UTR (WT - ncCPE)
Tex19.1 3'UTR (ΔCPE)
Luciferase Units (RLuc/FFLuc)
ns
ns
****
****
0 2 4 6 8 10 12 14 16 18
Time (hrs)
C
50
40
30
20
10
0
Tex19.1 3'UTR (WT-ncCPE)
Tex19.1 3'UTR (cCPE)
Luciferase Units (RLuc/FFLuc)
ns
ns
****
****
0 2 4 6 8 10 12 14 16 18
Time (hrs)

Figure 5

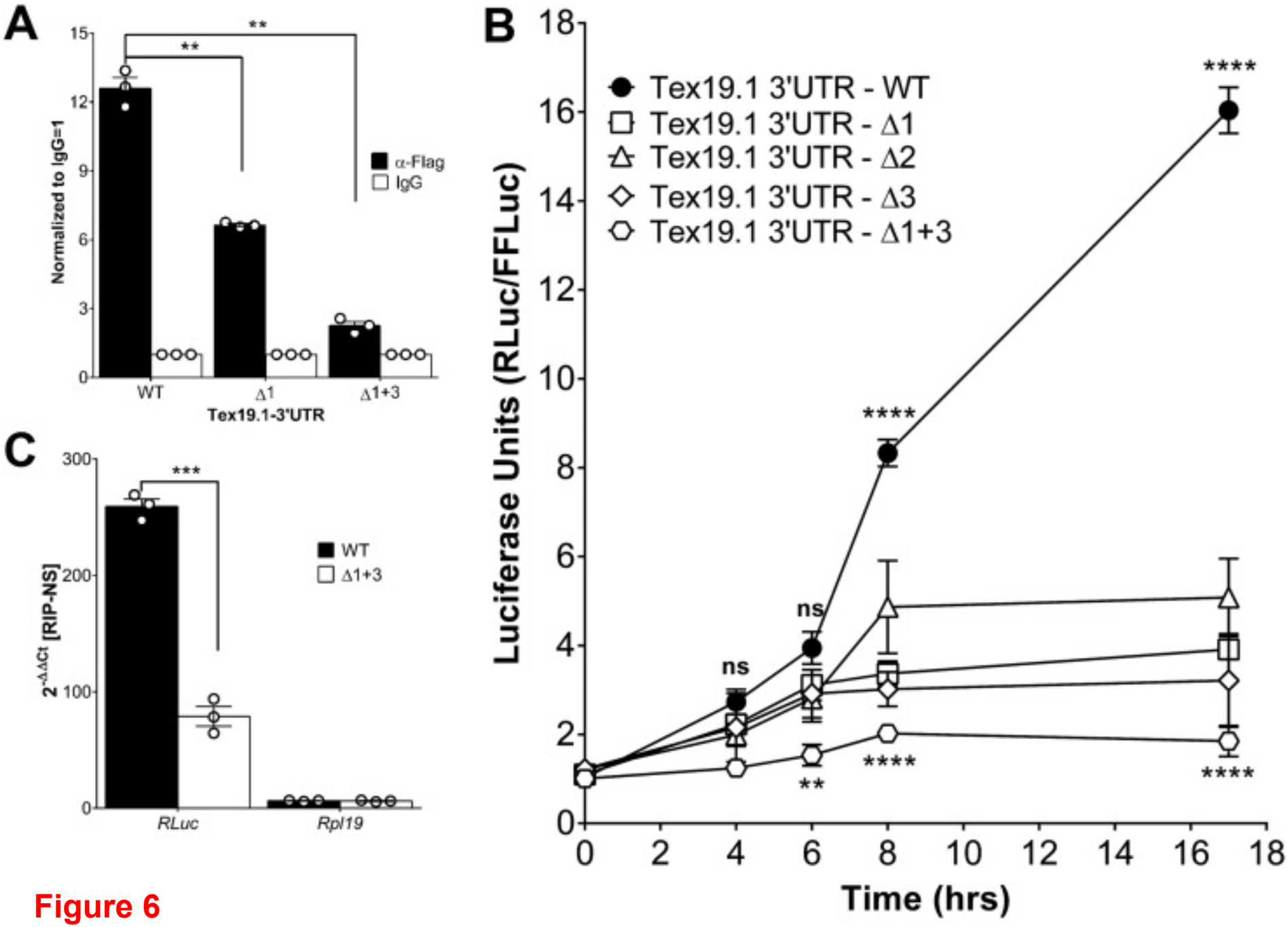
A
Normalized to IgG=1
α-Flag
IgG
WT
Δ1
Δ1+3
Tex19.1-3'UTR
B
Tex19.1 3'UTR - WT
Tex19.1 3'UTR - Δ1
Tex19.1 3'UTR - Δ2
Tex19.1 3'UTR - Δ3
Tex19.1 3'UTR - Δ1+3
Luciferase Units (RLuc/FFLuc)
Time (hrs)
ns
ns
**
****
****
****
C
2^-ΔΔCt [RIP-NS]
WT
Δ1+3
RLuc
Rpl19

Figure 6

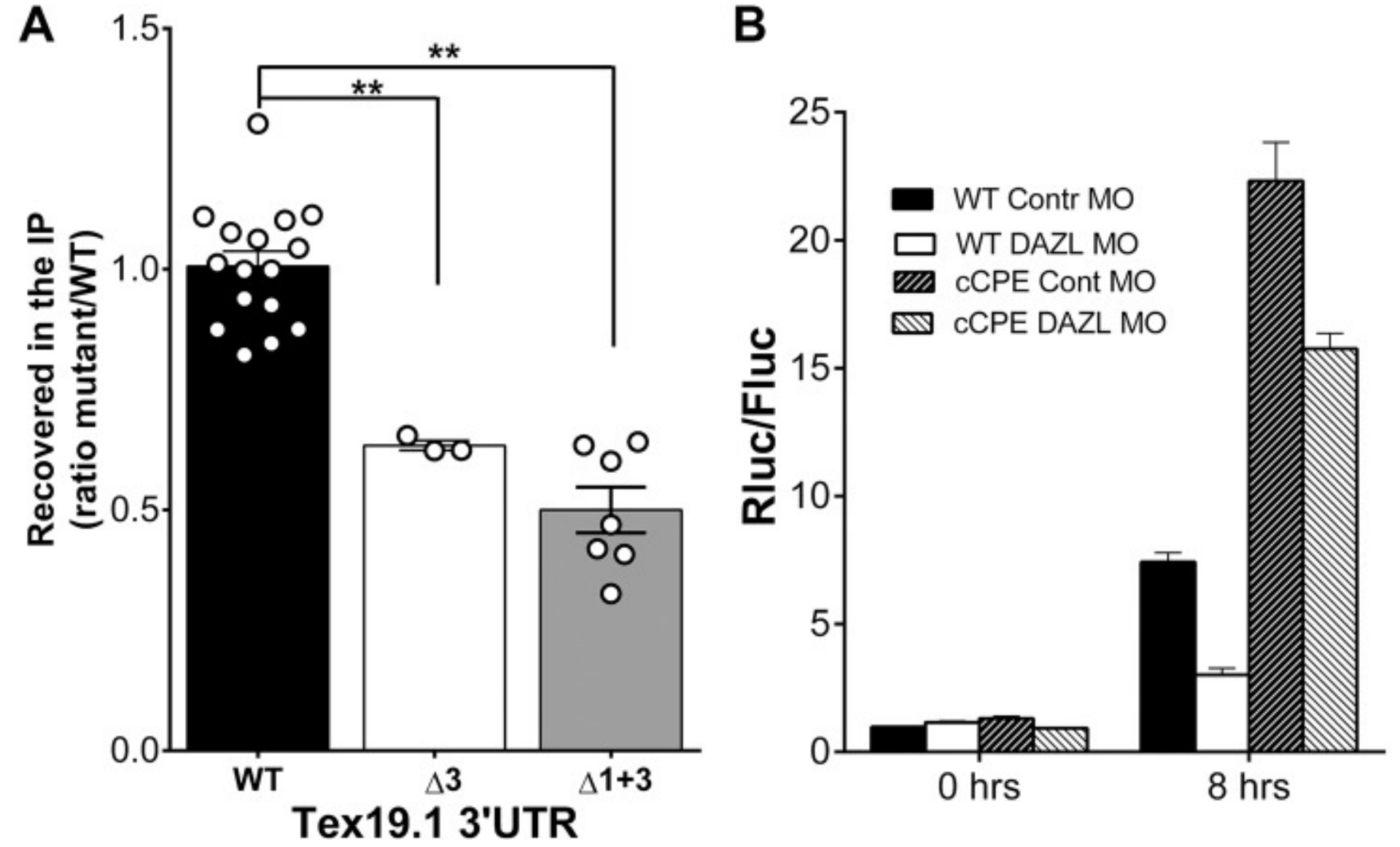
A
1.5
1.0
0.5
0.0
**
**
Recovered in the IP
(ratio mutant/WT)
WT
Δ3
Δ1+3
Tex19.1 3'UTR
B
25
20
15
10
5
0
Rluc/Fluc
WT Contr MO
WT DAZL MO
cCPE Cont MO
cCPE DAZL MO
0 hrs
8 hrs

Figure 7

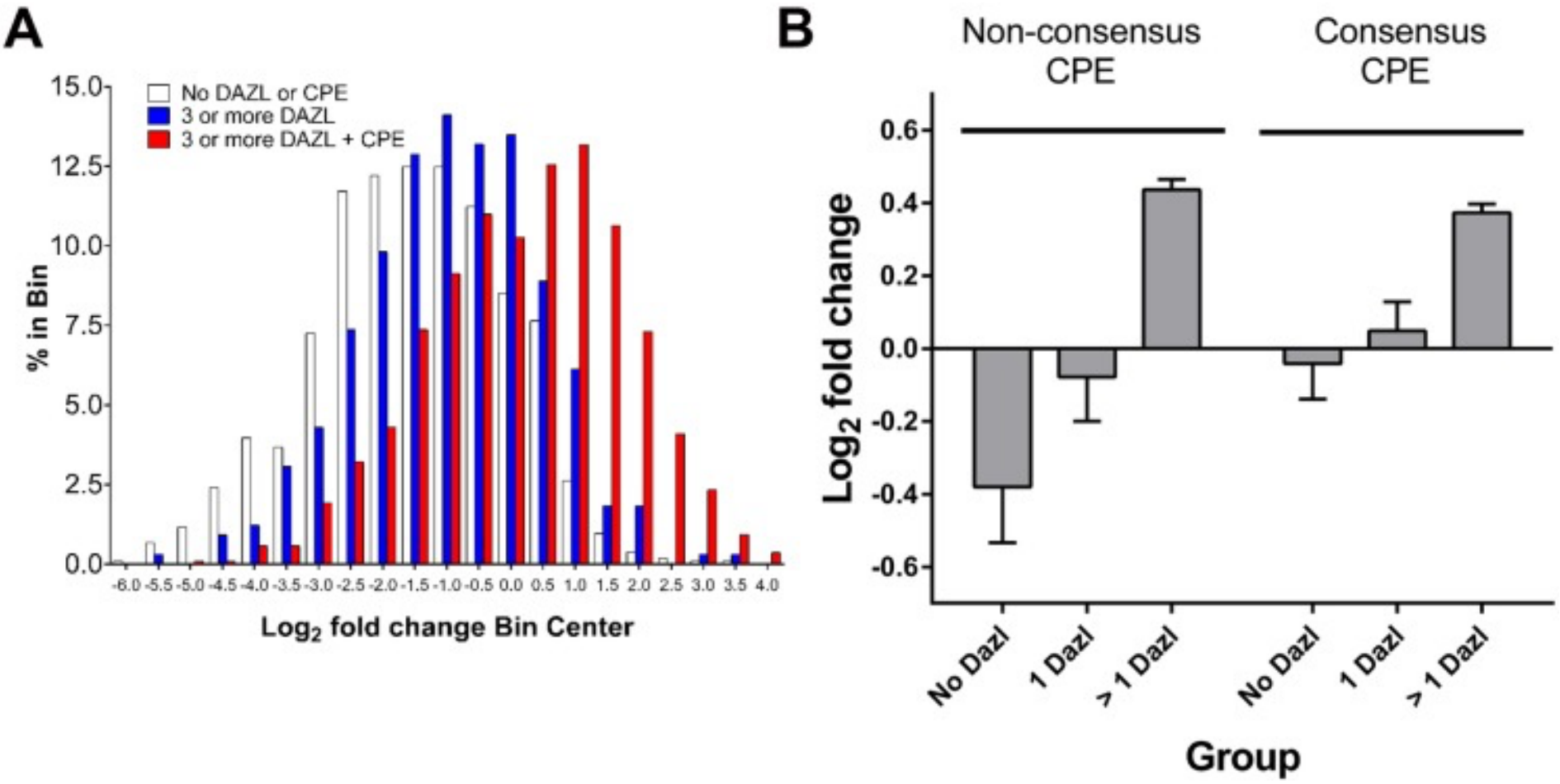
A
No DAZL or CPE
3 or more DAZL
3 or more DAZL + CPE
% in Bin
15.0
12.5
10.0
7.5
5.0
2.5
0.0
-6.0 -5.5 -5.0 -4.5 -4.0 -3.5 -3.0 -2.5 -2.0 -1.5 -1.0 -0.5 0.0 0.5 1.0 1.5 2.0 2.5 3.0 3.5 4.0
Log2 fold change Bin Center
B
Non-consensus CPE
Consensus CPE
Log2 fold change
0.6
0.4
0.2
0.0
-0.2
-0.4
-0.6
No Dazl
1 Dazl
> 1 Dazl
No Dazl
1 Dazl
> 1 Dazl
Group

Figure 8